

Electronics and Computer Science  
Faculty of Physical Sciences and Engineering  
University of Southampton

Adam Melvin

March 2018

# **Using Data Abstraction and Inter-Frame Interpolation for Low Data Rate Communication Between a 3D Camera and VR Headset**

Project supervisor: Klaus-Peter Zauner

Second examiner: Sheng Chen

A project progress report submitted for the award of  
MEng Electronic Engineering



UNIVERSITY OF SOUTHAMPTON

## *Abstract*

Faculty of Physical Sciences and Engineering  
Electronics and Computer Science

MEng Electronic Engineering

by Adam Melvin

The application of Virtual Reality (VR) to telerobotics is a current area of study in industry due to a desire for the increased spacial awareness VR provides. However, attempts to implement such a system using standard teleoperation techniques result in sub-par performance and an uncomfortable experience for the user; the benefits of a VR based system are entirely eliminated. The system proposed by this project incorporates elements of data abstraction and inter-frame interpolation to produce abstractions of the environment with lower performance requirements, as opposed to the standard approach of aiming for the presentation of an exact replica.



# Contents

<b>1</b>	<b>Introduction</b>	<b>1</b>
<b>2</b>	<b>Background</b>	<b>3</b>
2.1	Virtual Reality . . . . .	3
2.2	Telerobotics . . . . .	4
2.2.1	VR in Telerobotics . . . . .	4
2.3	Data Abstraction . . . . .	5
2.4	Inter-Frame Interpolation . . . . .	6
2.5	Sobol Sequences . . . . .	7
2.6	Computer Vision . . . . .	7
2.6.1	Edge Detection . . . . .	8
2.6.2	Flood Fill . . . . .	8
2.6.3	Depth Mapping . . . . .	9
<b>3</b>	<b>Abstraction Algorithm Development</b>	<b>11</b>
3.1	Edge Detection . . . . .	12
3.2	Flood filling . . . . .	13
3.2.1	Seed Point . . . . .	13
3.2.2	Fill Colour . . . . .	14
<b>4</b>	<b>Embedded Implementation</b>	<b>17</b>
<b>5</b>	<b>Server-Side Implementation</b>	<b>19</b>
<b>6</b>	<b>System Evaluation</b>	<b>21</b>
<b>7</b>	<b>Project Evaluation and Conclusion</b>	<b>23</b>
<b>A</b>	<b>Edge Detection Experimentation</b>	<b>25</b>
<b>B</b>	<b>Contour Based Seed Point Location</b>	<b>29</b>
<b>C</b>	<b>Demonstrations of Full Data Abstraction</b>	<b>31</b>

<b>D Gantt Chart</b>	<b>33</b>
<b>E Costing and Risk Assessment</b>	<b>35</b>
<b>Bibliography</b>	<b>37</b>

# List of Figures

2.1	HTC Vive . . . . .	3
2.2	Indirect VR teleoperations examples . . . . .	5
2.3	Data Abstraction Example . . . . .	6
2.4	Comparison of pseudo-random and quasi-random sequences . . . . .	7
2.5	Canny Edge Detection Example . . . . .	8
2.6	Example of Flood Fill . . . . .	9
3.1	Process of Edge Detection . . . . .	12
3.2	Comparison of brute force and Sobol seed point generation . . . . .	14
3.3	Comparison of Colour Averaging Methods . . . . .	16
A.1	The effect of blurring on edge detection . . . . .	25
A.2	The effect of changing Canny threshold values . . . . .	27
B.1	Demonstration of contour centre point location . . . . .	30
C.1	Demonstration of full abstraction process . . . . .	31
C.2	Additional examples of the full abstraction process . . . . .	32
E.1	Hardware Costs List . . . . .	35
E.2	Risk Assessment . . . . .	36



## *Acknowledgements*

I would like to thank Klaus-Peter Zauner and all the people who have had to put up with being constantly on camera for their patience. I would also like to thank Tom Darlison for allowing me access to his photographs.



# Chapter 1

## Introduction

There are many areas of science and engineering that require the observation of, and interaction with, environments not suitable for human beings. These environments are instead observed using teleoperated robots, potentially completely removing the need to put people in any danger. However, a challenge presented by telerobotics is giving the operator sufficient information about the robot's surroundings to give them a feeling of presence [1] within the space; this is essential for effective manoeuvring and interaction.

Virtual Reality (VR) is a technology that has proven itself to be able to provide the user with unparalleled presence within a virtual space- comparable to presence within a real, physical space [2, 3]. To be able to incorporate VR into teleoperation is therefore desirable. While this has been successfully attempted for the purpose of controlling robots within an already mapped space [4], there has been much less success in exploring an unknown space through a VR interface. This is due to the high frame rate and low latency required to prevent motion sickness while in a VR environment.

It's widely accepted that for a VR application to not cause motion sickness and headaches due to frame rate, it must maintain at least 90 frames per second (fps) [5]; a minimum of 60 fps can also be acceptable [6], but generally only for applications with little motion or when used by people with lower susceptibility to motion sickness. Unfortunately, to transmit 90 fps from a stereo camera rig (two images are required to perceive 3D) to the computer running the VR application has very high bandwidth

requirements. Also, a major factor in providing presence to the user in VR is their ability to look around the space independently. This can be achieved by mounting the stereo camera rig on a gimble, however to build a gimble that is able to track the angle of the user's head accurately and with low latency is both expensive and challenging [7]; if not implemented perfectly the user would be more likely to suffer sickness and dissociation from the space than if the gimble was not used at all.

The aim of this project was to design and implement a VR based teleoperation system that utilises data abstraction and inter-frame interpolation to minimise the outlined technical issues, providing increased comfort and therefore presence to the user than otherwise possible. Data abstraction would be used in the robot to reduce each image down to its most essential features, reducing its size and therefore the required data rate significantly. Each image pair would then transmitted to a server and combined into a single 3D map of the space that could be looked around freely through the VR headset. As the camera feed would be viewed as a 3D environment rather than directly as images, the headset could run at the full 90fps even if the environment is updating at a much slower rate. As previously suggested, a camera gimble would track the movement of the headset, but it would not have to be very accurate as it would only updating the 3D map and not affect the headset directly.

The system would be realised using off-the-shelf VR equipment, a camera gimble adapted from one produced by previous students [8], and a simple rover that I would also building.

# Chapter 2

## Background

### 2.1 Virtual Reality

The term Virtual Reality (VR) refers to the generation of a 3D environment that can be interacted with by a user in a realistic fashion, with the aim of immersing the user in the environment as if it were the real world [9]. While there are a large array of systems that can be considered VR, whenever the term is used in this report it is only referring to the head-mounted display (HMD) systems that have become popular in recent years with the release of the Oculus Rift [10] and the HTC Vive [11] (Figure 2.1); these are both consumer grade systems that are aimed at the immersive gaming market.



FIGURE 2.1: HTC Vive. Pictures of the Vive headset, reproduced from [11].

HMD based systems display different images for each eye to provide the user with a sense of depth within the 3D environment, making the headset effectively operate like a pair of binoculars into the virtual world. The headset is also tracked in 3D space, and this movement translated into the 3D environment with very low latency. These features, among others, are all implemented with the aim of providing the user with presence within the virtual space that is comparable to observing the real world.

Due to its availability at the University of Southampton and in my own home, the HTC Vive was used as the VR device in the implementation of the teleoperations system discussed in this report.

## 2.2 Telerobotics

As discussed in the introduction, a telerobot is a robot controlled from a distance by a human operator [12]. Telerobots are typically developed to undertake activities within environments that are too dangerous or costly for humans to work in, an example being the extensive telerobotics research at NASA for tasks such as deep-space exploration [13].

### 2.2.1 VR in Telerobotics

The use of HMDs in teleoperations is not a new concept; NASA's Robonaut 2 was sent to the International Space Station in 2011 and can be controlled through a headset that displays the output of the robot's head cameras [14], and flying drones by First Person View (FPV), an analogue video feed transmitted over radio to a HMD, is very popular [15]. However, these systems are either incredibly expensive (Robonaut 2 is worth millions of dollars) or very limited (FPV systems send one, low quality, video stream over a short distance), and all have the motion sickness issues discussed in the introduction. While stereo camera FPV systems have been developed, so the user has depth perception and better presence in the drone's view, the motion sickness problem remains the major drawback of HMD based teleoperations systems [16].

As previously established, motion sickness in VR is mitigated through high frame rates and low latency. However, most VR based teleoperations systems currently available are direct VR systems, so they display the video feeds produced from the device's cameras directly in the headset. This entirely ties the frame rate and latency of the headset to the capabilities of the video transmission system, and only the most expensive and complicated systems will meet the strict requirements for comfortable VR.

An alternate option to a direct system is an indirect system. This is one in which the video feed is abstracted from the headset in some way in the hope of providing improved comfort and awareness. Indirect systems can come in a variety of forms, such as a virtual control room with the video feed on a virtual screen [17], or a 3D map generated from a multi-line LiDAR and IMU [18] (Figure 2.2). These examples show the potential of indirect systems as a solution to VR based teleoperations, though the research into this field is currently minimal; this project aims to expand on this research with the development of its novel system.

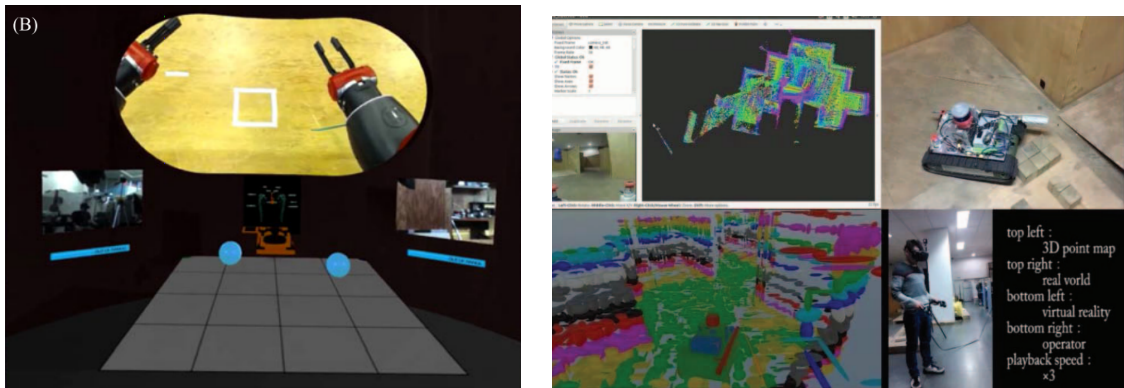


FIGURE 2.2: Indirect VR teleoperations examples. A virtual control room based system (left) and a LiDAR 3D map based system (right), reproduced from [17] and [18].

## 2.3 Data Abstraction

”Data abstraction” is the phrase that will be used in this report to describe the act of reducing an image down to only its most essential elements. It is similar in concept to an artist sketching a scene instead of attempting a full drawing, and is

comparable to data compression as the aim is also to reduce the file size of the image, however data abstraction takes a very different approach to solving the problem than standard compression algorithms.

Data compression is the storing of information using a more space efficient encoding [19]. While some information is lost during lossy compression, the aim regardless of the algorithm used is to retain as much of the original information as possible. In contrast, the aim when utilising data abstraction is to discard all the information that is unnecessary to fulfilling the image's purpose. For example, if all that is required of an image is that basic shapes can be identified, then only the information on the boundaries of the shapes is necessary; the rest of the image can be discarded. An implementation of data abstraction can be seen in Figure 2.3.

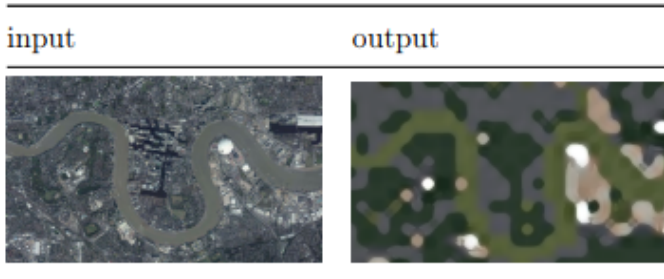


FIGURE 2.3: Data Abstraction Example. This is the abstraction of an aerial photograph of London, reproduced from [20]

## 2.4 Inter-Frame Interpolation

Inter-frame interpolation is the generation of intermediate frames in a video feed to increase its frame rate. This is typically done using estimations of optical flow to interpolate frames within a pre-recorded sequence [21], though there are methods that can achieve real-time video processing when provided with powerful enough hardware [22]. In this report, the term inter-frame interpolation refers to the increase in frame rate provided by the conversion of the video feed into a 3D map, as in effect we are interpolating the <30fps video feed up to 90fps in the VR headset.

## 2.5 Sobol Sequences

Sobol sequences are quasi-random sequences that were introduced to aid in approximating integrals. The aim is to form a sequence of points that are evenly spread across an S-dimensional unit cube [23]. This provides a much more even spread of points across the chosen space than can be produced from a pseudo-random number source (Figure 2.4). The code used in this project to produce these sequences was created by Leonhard Grünschloß [24].

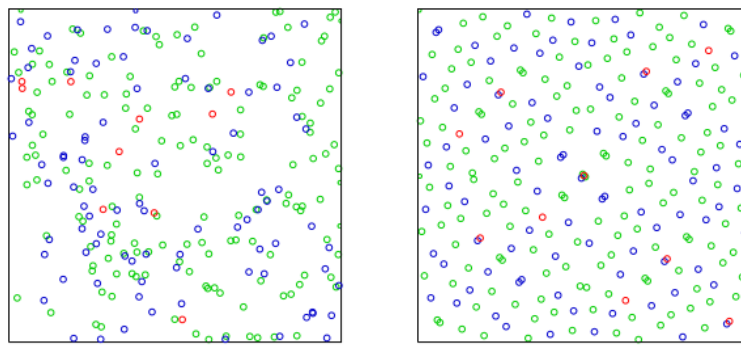


FIGURE 2.4: Comparison of pseudo-random and quasi-random sequences. 256 points from a pseudo-random generator (left) and 256 points from a Sobol sequence (right), reproduced from [25].

## 2.6 Computer Vision

Computer vision is the automatic analysis of images and extraction of the useful information they contain [26]. A raw image is simply a large matrix of colour values, so for a computer to take action based on the contents of an image it must be able to recognise features using analysis of this data. Doing so involves many different techniques such as statistical pattern classification and geometric modelling [27]. All computer vision methods in this project are implemented using the OpenCV libraries, and the example programs provided with them used as starting points for development [28].

### 2.6.1 Edge Detection

When attempting to recognise the features of an image, knowing the locations of the edges of objects within the scene is often very useful. An edge is defined as a significant local change in intensity, usually due to a discontinuity in either the intensity or its first derivative [29]. There are many algorithms available that will detect the edges of an image from the locations of these discontinuities. When the most popular algorithms (Laplacian of Gaussian, Robert, Prewitt, Sobel, and Canny) are compared [30], the most effective in almost all scenarios is Canny edge detection [31], therefore this is the algorithm utilised in this project. Canny edge detection is demonstrated in Figure 2.5.

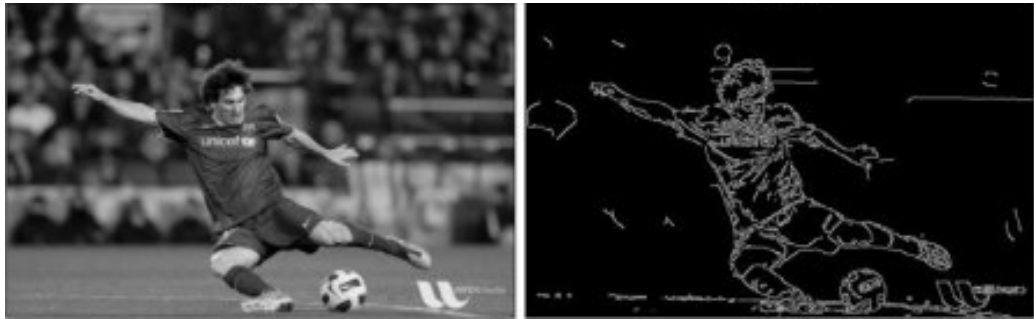


FIGURE 2.5: Canny Edge Detection Example. Simple edge detection program applied to a fairly detailed photo of Messi, to demonstrate its effectiveness even with more complex images. Figure taken from an OpenCV Canny tutorial [32].

### 2.6.2 Flood Fill

Flood fill algorithms determine the area connected to a given cell (the seed point) in a multi-dimensional array that have similar intensity values for the purpose of filling them with a chosen colour [33]. This is a technique that is not only useful in image processing, but also for many other fields such as in passive acoustic monitoring where finding the area connected to a given node can be useful as part of tracking in 4D space (x,y,z,time) [34]. A demonstration of flood fill has been presented in Figure 2.6.

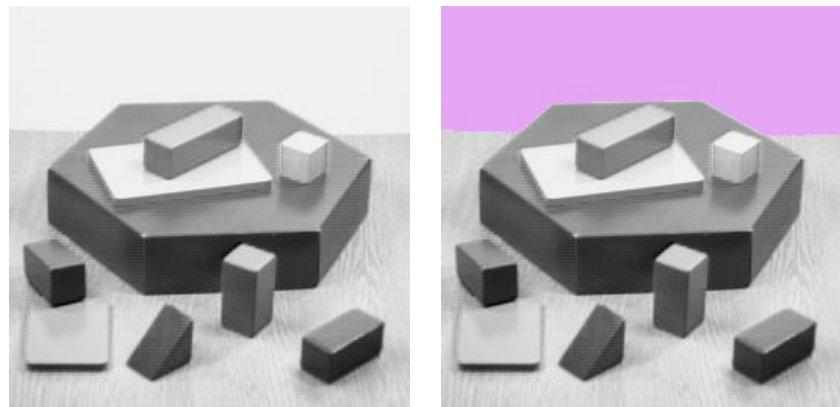


FIGURE 2.6: Example of Flood Fill. The original image (left) was provided by OpenCV. The right image is the result of flood filling from the top left corner.

### 2.6.3 Depth Mapping



# Chapter 3

## Abstraction Algorithm Development

In this implementation of data abstraction, the aim is to reduce images down to only the boundaries of the objects in the scene and then fill the spaces between these boundaries with block colours based on the original image. Therefore the general process of the design is:

1. Use edge detection on the image, presenting the boundaries of the scene as white lines and the rest as black.
2. Divide up the original image into sections that can reasonably be averaged into a single colour, defined by the boundaries produced by the edge detection or otherwise.
3. Find the average colours (or reasonable alternatives) for these sections.
4. Flood fill the spaces in the edge detection output with the average colours of the original image.

While this section will be presented in the context of the entire process occurring on a single computer (as this was the testing platform), when incorporated into the final system points 1-3 will be done using the raspberry pi on the rover and point 4 will be done on the computer. This allows for much smaller data packets to be sent

over a wireless connection (wifi), due to being able to send the colour information for entire sections of the image as a single colour value.

### 3.1 Edge Detection

Canny edge detection was implemented using the Canny function provided by OpenCV. The sequence of processes implemented to support the algorithm in producing high quality edges are shown in Figure 3.1.

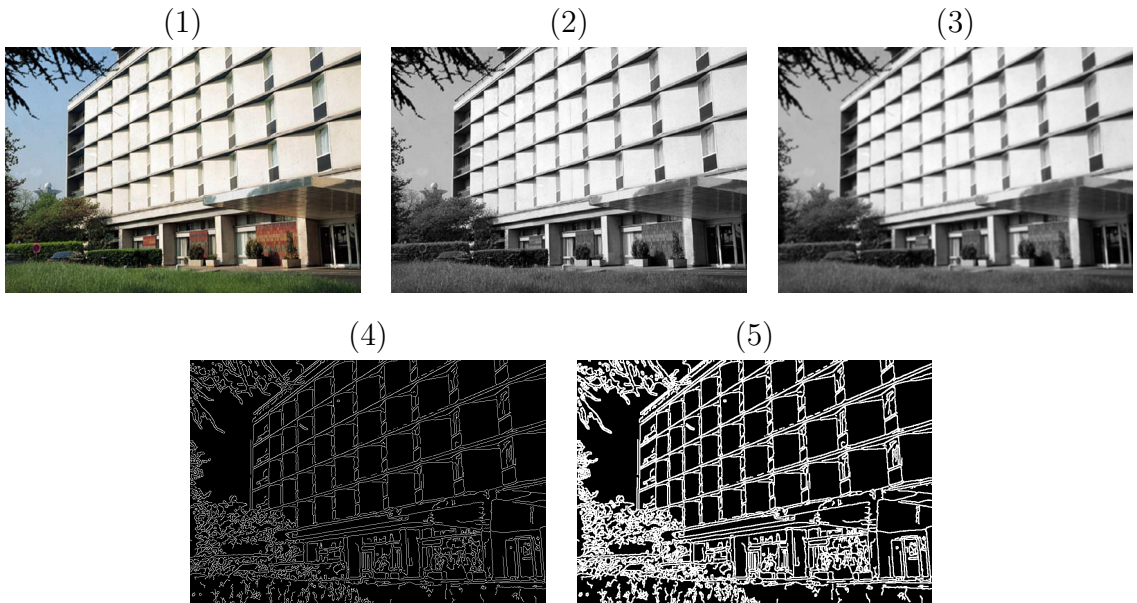


FIGURE 3.1: (1) the original image, provided by OpenCV, (2) post grayscaling, (3) post blurring, (4) post edge detection, and (5) post dilation.

The image is first made grayscale, as Canny detects large changes in light intensity and not colour. The image is then blurred to remove any unnecessary edges and noise that Canny may pick up. The edge detection is used, producing white lines representing the edges on a black background (the details of parameter experimentation with Canny and the previous blurring are presented in Appendix B). The output of the edge detection is finally dilated to make the lines thicker and bridge the gaps between the lines that are very close together. This is done to make the

image more cartoon-like and more generally aesthetically pleasing, reduce the number of lines produced by areas that are dense with detail such as hair and foliage (an example of this detail density can be seen in the bush in Figure A.1), and to bridge the gaps between lines that are close together, increasing the likelihood of defined shapes being created that can be easily flood filled later.

## 3.2 Flood filling

Flood filling was chosen as the method for applying colour to the Canny output image, as it is the most efficient way to fill spaces of unknown size and shape that are defined by high contrast boundaries; using it makes dividing up the image into sections unnecessary. To use the OpenCV flood fill function you must provide a seed point to start flooding from, a colour to fill with, and parameters for the filling itself (unchanged from the defaults provided by the OpenCV documentation [35]).

### 3.2.1 Seed Point

Finding the points to flood fill from is a challenge, as each image will have a different number of spaces to be filled and the spaces can be anywhere. Three different methods were attempted to solve the problem. The first was an attempt to use OpenCV's contour functionality to provide seed points, however this was unusable due to high resource requirements. The method is detailed in Appendix C.

Although it would be ideal to aim to flood fill from the centre point of each space, it is only necessary if a few specific pixels are being selected to fill from, as each time a line pixel is selected that potential seed point can only be discarded. It is possible to instead iterate through the whole image and flood fill from every pixel found that is not part of a line or an already filled space.

This method is more effective at filling every space than the previous, and is also less resource intensive. However, if presented with a complicated environment with many spaces to flood fill, it must fill every single one, therefore leading to unacceptable drops in frame rate.

The most simple solution to the performance issues caused by allowing the number of times flood fill is used per image to vary would be to set a maximum. However, if this is done the seed points can no longer be selected by iterating through the whole image, as the presence of many small spaces at the top of an image would lead to larger, more important spaces not being filled at the bottom. The solution is to select a set number of points quasi-randomly across the image using Sobol sequencing. Although a certain number of points will land on lines and therefore not be used, if there are enough points then all the important spaces are filled without serious impact on performance. Also, with this method performance is not affected by the complexity of the image, however more complicated images will be processed with many of the more dense areas unfilled (Figure 3.2). For these reasons, the seed points are selected using this method in the current build.

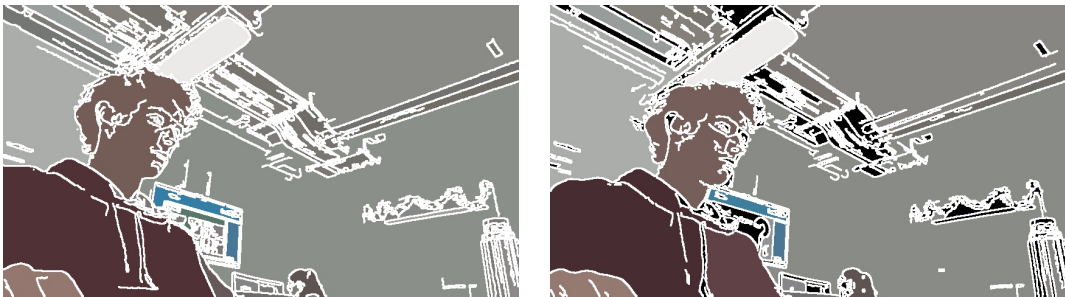


FIGURE 3.2: Comparison of brute force and Sobol seed point generation. It can be clearly seen that the brute force method (left) accurately fills every space in the image, whereas using Sobol results in many unfilled spaces. However, Sobol is higher performance with a frame rate of 17.14fps, compared to 8.57fps using brute force.

### 3.2.2 Fill Colour

Three different methods were considered for finding the colours that the Canny output should be flood filled with. All three methods are valid solutions, but present different ratios between accuracy and resource requirements.

While filling the abstracted image with the average colours present within the input is preferable, it is not essential to the project; provided that the objects in the scene are still recognisable, they don't have to be exactly the right colour. For this reason it would be acceptable to not find the average colour of the area being flood filled

at all, and instead simply use the colour of the seed point. This is a very fast method, however produces incredibly inconsistent colours between images. This is because there can be a wide spectrum of colour across a single surface even within the threshold of Canny edge detection, and the Sobol sequence will sample from a different point each time producing spaces that flicker between a wide range of colours.

The consistency of the previous method can be improved substantially with minimal impact on performance by taking an average of the colour within the area of a small circle around the seed point, rather than just the colour of that one point. This significantly improves the consistency between images, however introduces the problem of incorporating pixels from outside the space to be filled. This is due to the quasi-random points often being closer to the edge of the space that they are being flooded from than the radius of the circle. Therefore, the size of the circle must be carefully selected to balance the benefits of increasing size (more consistency when the seed point is further from the edge) and the benefits of decreasing size (more consistency when the seed point is closer to the edge).

The OpenCV flood fill function provides the ability to fill a blank mask using the boundaries defined by a different image [36]. This makes it possible to create a custom mask with the exact size and shape of the space that is to be filled and use that to find the average colour instead of the predefined circle. This produces the average colour of every space in the image exactly at the expense of adding an extra stage of flood filling before the Canny output itself is filled. The consistency between images for this is the maximum possible based on colour alone (Figure 3.3), though inconsistency in the edge detection causes certain spaces to combine and divide constantly, leading to a small amount of colour inconsistency to remain regardless. This method has a noticeable impact on performance, though within acceptable bounds, leading this to be the chosen method for the current build. Examples of the results produced by the final build can be seen in Appendix D.

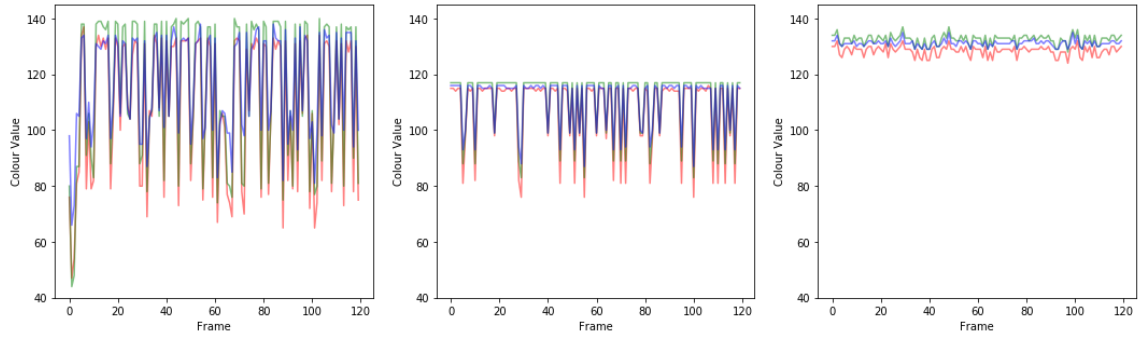


FIGURE 3.3: Comparison of Colour Averaging Methods. These are RGB values over time produced by flood filling an example area using the seed point colour (left), circle average (middle), and flood fill average (right). The increase in consistency from left to right is very apparent.

# Chapter 4

## Embedded Implementation



# **Chapter 5**

## **Server-Side Implementation**



# **Chapter 6**

## **System Evaluation**



## **Chapter 7**

# **Project Evaluation and Conclusion**



# Appendix A

## Edge Detection Experimentation

The effect of changing the size of the blur kernel was tested (Figure A.1), and it was determined that the size of the kernel has a slight effect on both the noise and edge accuracy; reducing the size makes the edges more accurate to the original at the expense of more noise, whereas increasing the size results in less noise but also less accurate edges.



FIGURE A.1: The effect of blurring on edge detection. From left to right the size of the square blur kernel is increasing through 3, 5, and 7, and the lower canny threshold is decreasing through 44, 26, and 18 (the threshold change was for the purpose of presenting the best case ratio of detail to noise for each image). This figure shows the minor decrease in noise as the blur kernel increases in size, but also the minor decrease in edge accuracy; this can be seen most clearly in the bush in the bottom right of the frame for noise, and the panels on the upper right of the building for edge accuracy

The edge detection function itself has 3 parameters- low threshold, high threshold, and kernel size. The kernel was set to 3x3 and the high threshold set to 3 times

the low threshold by the recommendation of the OpenCV documentation [37]. From there the effect of changing the low threshold was tested (Figure A.2). Increasing the threshold increased the level of detail at the expense of also increasing the noise. However, it was discerned that different situations can call for drastically different thresholds, therefore necessitating the ability to change the threshold at runtime from within the Unreal 4 environment.

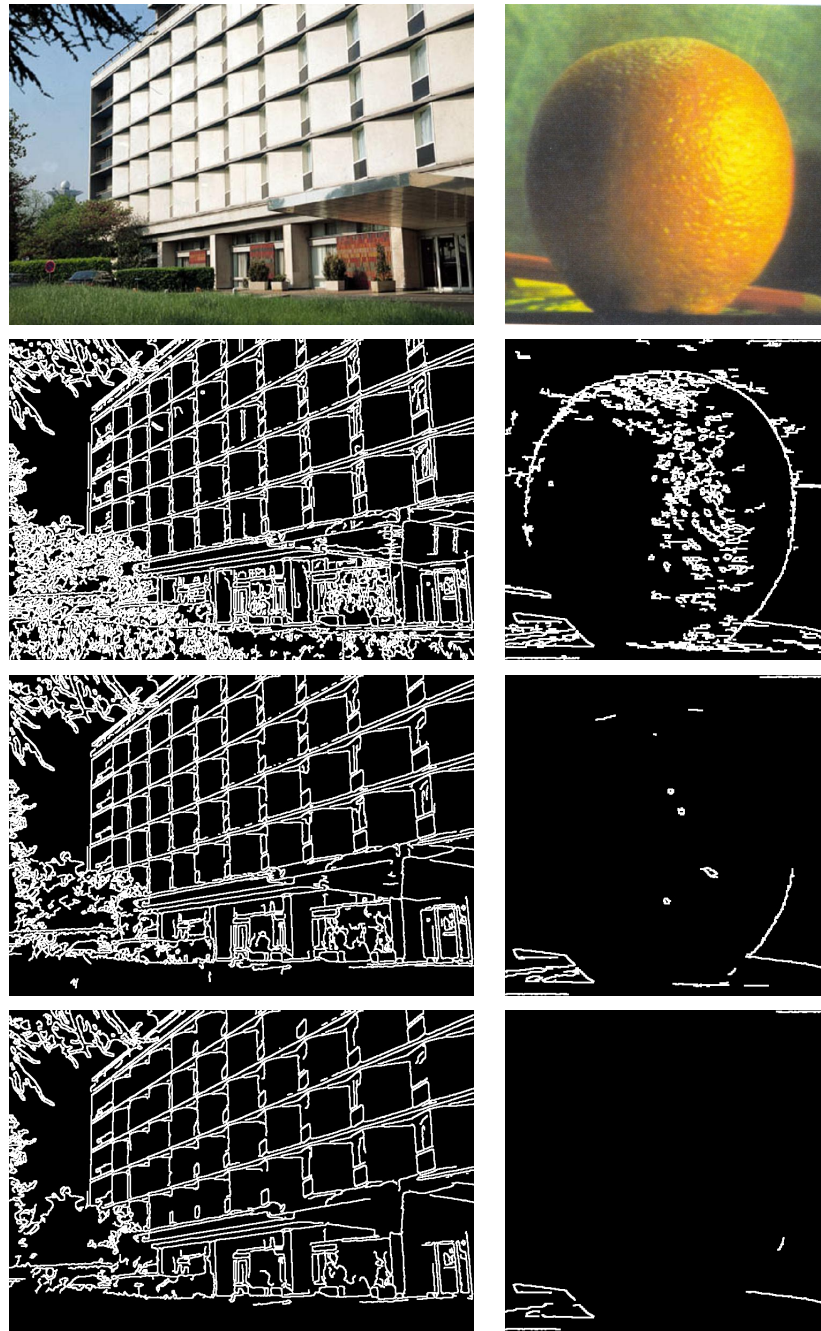


FIGURE A.2: The effect of changing Canny threshold values. From top to bottom, presented are images provided by OpenCV, then those images edge detected with low thresholds of 15, 30, and 45. The blur kernel is always 5x5 and the high threshold 3 times the low threshold. It can be seen that the best threshold for the building is 30, whereas the best for the orange is 15. This proves the necessity of being able to change the threshold at run-time to account for different situations.



# Appendix B

## Contour Based Seed Point Location

The ideal place to aim to flood fill a space from would be the centre point of the space. OpenCV provides the functionality to take the Canny output image (a matrix of colour values) and convert it into a set of contours. Contours are line objects stored in a hierarchical structure and have functions that can provide the centre point of each contour. Although the centre points of the contours will not map exactly to the centre points of the space, they are close enough approximations to flood fill from (Figure B.1).

Unfortunately, due to a combination of the processing time required to convert the lines into contours and the number of contours produced that have no impact on the spaces left to be flood filled, this method is too resource heavy to produce 10 fps on a laptop, therefore is also too resource heavy for use on the raspberry pi.

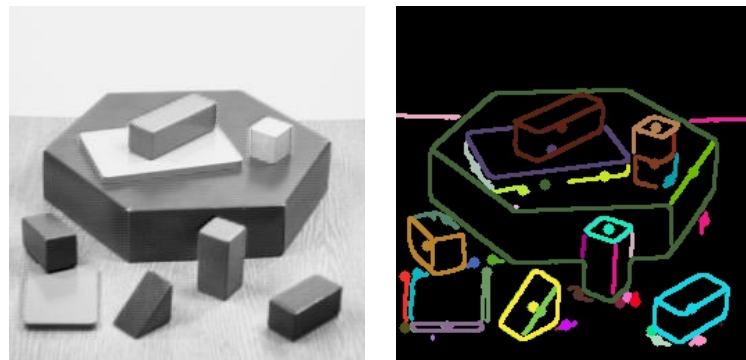


FIGURE B.1: Demonstration of contour centre point location. The original image (provided by OpenCV) on the left has been Canny edge detected, these edges have converted into contours, and the centre points of these contours located. The results of this are displayed on the right, with each contour and its corresponding centre point in a different colour. It can be observed that the centre points provide adequate coverage of the black spaces in the image to be used as seed points for flood filling.

# Appendix C

## Demonstrations of Full Data Abstraction



FIGURE C.1: Demonstration of full abstraction process. The final parameters and methods (of those under discussion) are a blur kernel of 5x5, a low threshold of 25 (for this example), Sobol seed point generation, and averaging via preliminary flood fill. It can be seen that most areas of the image are being effectively edge detected and flood filled with the correct colours; however, some areas are hard to interpret such as around the bushes in the bottom left, and some spaces have been left unfilled such as the panel below the top left corner of the building. These issues are minimal though, therefore leading me to conclude that the process is effective at producing recognisable abstractions of the input images.

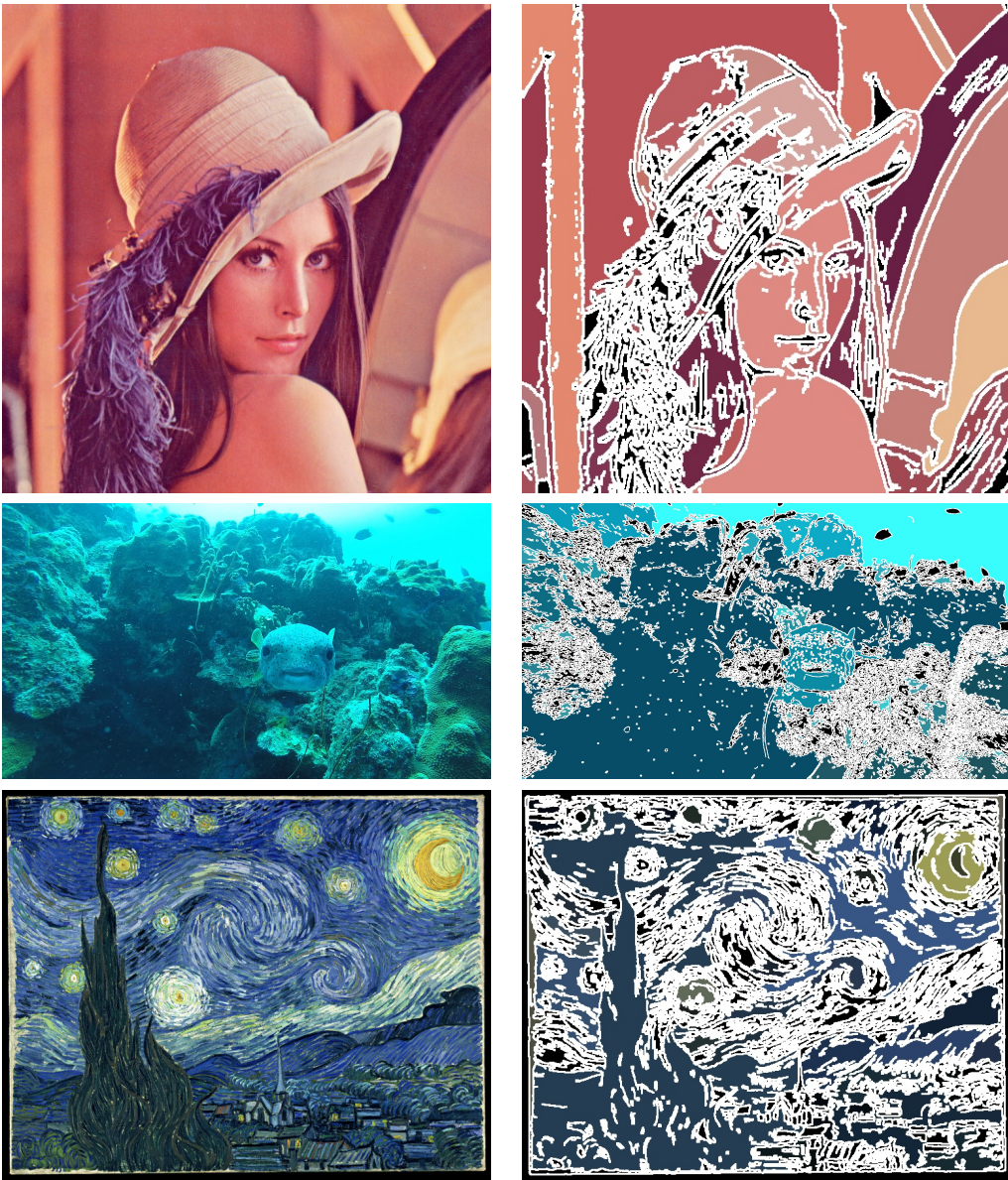
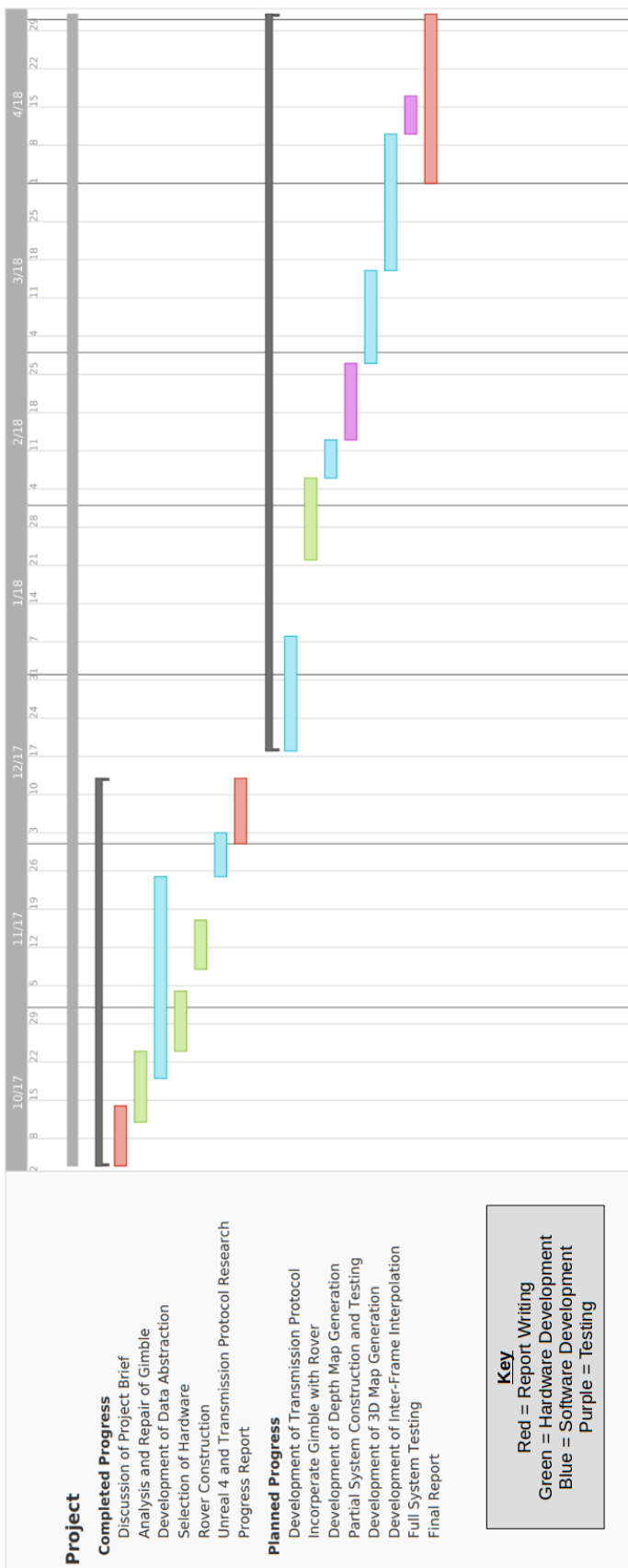


FIGURE C.2: Additional examples of the full abstraction process. The top image (provided by OpenCV) is very simple, so the abstraction gives clean and easily recognisable results. The middle image (provided by fellow student Tom Darlison) was selected due to its limited colour palette and poor focus to test the limits of the process. While the image has mostly filled to a single colour, the pufferfish, rocks, coral, background fish, and open water are all identifiable. The bottom image (provided by OpenCV) was selected due to the extreme number of edges, due to the very clear brush strokes. Once the Canny threshold was turned down considerably, the result was recognisable as Starry Night, though much of the image has been overwhelmed by the edge detection lines. It can be concluded from these tests that the data abstraction process is effective at producing recognisable images, however the difficulty in interpreting the abstracted images is heavily dependant on the focus and complexity of the image.

# **Appendix D**

## **Gantt Chart**



## Appendix E

### Costing and Risk Assessment

Component	Supplier	Price	Quantity	Delivery
Edimax USB 2.0 Wireless Adapter	RS	£17.05	1	£0.00
Nylon XT60 Connectors Male/Female (5 pairs)	Hobby King	£3.00	1	
XT60 Harness for 2 Packs in Parallel	Hobby King	£1.94	1	
GEP-XT60 PDB BEC 5V & 12V	Hobby King	£3.04	1	£4.66
Turnigy 2650mAh 4S 20C Lipo Pack	Hobby King	£12.28	2	
MAX14870 Single DC Motor Driver Carrier	HobbyTronics	£5.40	2	£2.88
HS1177 Sony Super HAD II CCD FPV Camera	Unmanned Tech	£21.00	2	£3.50
Black EasyCAP USB Video Adapter	GearBest	£11.29	2	£0.00

FIGURE E.1: Hardware Costs List. This shows the use of budget for this project thus far. Total budget spent = £124.97

Risk Event	Likelihood (1-5)	Impact (1-5)	Risk Exposure (1-25)	Action
Unable to complete system in time	4	4	16	System is built from the input to the output, allowing for the submission of the working section instead
Response time of the system is unacceptable for use in VR	3	5	15	System is designed and being build with runtime performance as the highest priority
Inter-frame interpolation does not perform as intended	3	3	9	System can function without this component
Data abstraction process is not accurate enough to form a depth map from	2	4	8	Areas where refinement is possible are known so the process can be made more accurate if necessary
EasyCap devices are never available or do not work with the Raspberry Pi	4	2	8	Preparations have been made to use my supervisor's budget to replace FPV cameras with webcams
Data abstraction process is too resource intensive for the Raspberry Pi	2	3	6	Areas where quality reductions could be made in exchange for performance are known
LiPo battery combusts	1	4	4	LiPo batteries are supervised while charging, charged in a flame-retardant bag, and only connected in parallel when the same voltage
Hardware failure	1	2	2	Remaining budget can be used to replace failed component

FIGURE E.2: Risk Assessment for the project going forward.

# Bibliography

- [1] K. M. Lee, “Presence, explicated,” *Communication Theory*, vol. 14, no. 1, pp. 27–50, 2004.
- [2] J. M. Loomis, “Presence in virtual reality and everyday life: Immersion within a world of representation,” *PRESENCE: Teleoperators and Virtual Environments*, vol. 25, no. 2, pp. 169–174, 2016.
- [3] S. A. McGlynn and W. A. Rogers, “Considerations for presence in teleoperation,” in *Proceedings of the Companion of the 2017 ACM/IEEE International Conference on Human-Robot Interaction*, HRI ’17, (New York, NY, USA), pp. 203–204, ACM, 2017.
- [4] M. Bounds, B. Wilson, A. Tavakkoli, and D. Loffredo, “An integrated cyber-physical immersive virtual reality framework with applications to telerobotics,” in *International Symposium on Visual Computing*, pp. 235–245, Springer, 2016.
- [5] IrisVR, “The importance of frame rates,” 2017. Available: <https://help.irisvr.com/hc/en-us/articles/215884547-The-Importance-of-Frame-Rates>. [Accessed: March 2018].
- [6] M. Borg, S. S. Johansen, K. S. Krog, D. L. Thomsen, and M. Kraus, “Using a graphics turing test to evaluate the effect of frame rate and motion blur on telepresence of animated objects,” in *GRAPP/IVAPP*, 2013.
- [7] E. Ackerman, “Oculus rift-based system brings true immersion to telepresence robots,” 2015. Available: <http://spectrum.ieee.org/automaton/robotics/robotics-hardware/upenn-dora-platform>. [Accessed: March 2018].

- [8] M. Gupta, F. Hennecker, T. Isaacs, M. Sharhan, and L. Stauskis, “Biologically inspired robots: A vision system inspired by the human eye,” 2016. Electronics and Computer Science, University of Southampton.
- [9] Virtual Reality Society, “What is virtual reality?,” 2017. Available: <https://www.vrs.org.uk/virtual-reality/what-is-virtual-reality.html>. [Accessed: March 2018].
- [10] Oculus, “Oculus rift homepage,” 2017. Available: <https://www.oculus.com/rift/>. [Accessed: March 2018].
- [11] HTC, “Htc vive homepage,” 2017. Available: <https://www.vive.com/uk/>. [Accessed: March 2018].
- [12] N. R. Council, *Virtual Reality: Scientific and Technological Challenges*. Washington, DC: The National Academies Press, 1995.
- [13] T. Fong, “Interactive exploration robots: Human-robotic collaboration and interactions,” 2017.
- [14] NASA, “Robonaut 2 homepage,” 2016. Available: <https://robonaut.jsc.nasa.gov/R2/>. [Accessed: March 2018].
- [15] RCExplorer, “Fpv starting guide,” 2009. Available: <https://rcexplorer.se/educational/2009/09/fpv-starting-guide/>. [Accessed: March 2018].
- [16] N. Smolyanskiy and M. Gonzalez-Franco, “Stereoscopic first person view system for drone navigation,” *Frontiers in Robotics and AI*, vol. 4, p. 11, 2017.
- [17] J. I. Lipton, A. J. Fay, and D. Rus, “Baxter’s homunculus: Virtual reality spaces for teleoperation in manufacturing,” *IEEE Robotics and Automation Letters*, vol. 3, no. 1, pp. 179–186, 2018.
- [18] P. Wang, J. Xiao, H. Lu, H. Zhang, R. Yan, and S. Hong, “A novel human-robot interaction system based on 3d mapping and virtual reality,” in *Chinese Automation Congress (CAC), 2017*, pp. 5888–5894, IEEE, 2017.
- [19] O. MAHDI, M. Alshujeary, and A. Jasim Mohamed, “Implementing a novel approach an convert audio compression to text coding via hybrid technique,” 11 2013.

- [20] A. Barrett-Sprot, “Data abstraction for low-bandwidth communication,” 2017. BEng Project Report, Electronics and Computer Science, University of Southampton, Available: [https://secure.ecs.soton.ac.uk/notes/comp3200/e\\_archive/COMP3200/1617/abs1g14/pdfs/Report.pdf](https://secure.ecs.soton.ac.uk/notes/comp3200/e_archive/COMP3200/1617/abs1g14/pdfs/Report.pdf). [Accessed: March 2018].
- [21] J. Ribas-Corbera and J. Sklansky, “Interframe interpolation of cinematic sequences,” *Journal of Visual Communication and image representation*, vol. 4, no. 4, pp. 392–406, 1993.
- [22] W. Shi, J. Caballero, F. Huszár, J. Totz, A. P. Aitken, R. Bishop, D. Rueckert, and Z. Wang, “Real-time single image and video super-resolution using an efficient sub-pixel convolutional neural network,” in *Proceedings of the IEEE Conference on Computer Vision and Pattern Recognition*, pp. 1874–1883, 2016.
- [23] S. Joe and F. Y. Kuo, “Constructing sobol sequences with better two-dimensional projections,” *SIAM Journal on Scientific Computing*, vol. 30, no. 5, pp. 2635–2654, 2008.
- [24] L. Grünschloß, “gruenschloss.org,” 2017. Available: <http://gruenschloss.org/>. [Accessed: March 2018].
- [25] Wikipedia, “Sobol sequence,” 2017. Available: [https://en.wikipedia.org/wiki/Sobol\\_sequence/](https://en.wikipedia.org/wiki/Sobol_sequence/). [Accessed: March 2018].
- [26] BMVA.org, “What is computer vision?,” 2017. Available: <http://www.bmva.org/visionoverview>. [Accessed: March 2018].
- [27] D. H. Ballard and C. M. Brown, “Computer vision,” *Prenice-Hall, Englewood Cliffs, NJ*, 1982.
- [28] OpenCV team, “Opencv,” 2017. Available: <https://opencv.org/>. [Accessed: March 2018].
- [29] R. Jain, R. Kasturi, and B. G. Schunck, *Machine vision*, vol. 5. McGraw-Hill New York, 1995.
- [30] R. Maini and H. Aggarwal, “Study and comparison of various image edge detection techniques,” *International journal of image processing (IJIP)*, vol. 3, no. 1, pp. 1–11, 2009.

- [31] J. Canny, “A computational approach to edge detection,” *IEEE Transactions on pattern analysis and machine intelligence*, no. 6, pp. 679–698, 1986.
- [32] A. Mordvintsev and K. Abid, “Opencv canny edge detection tutorial,” 2013. Available: [http://opencv-python-tutorials.readthedocs.io/en/latest/py\\_tutorials/py\\_imgproc/py\\_canny/py\\_canny.html](http://opencv-python-tutorials.readthedocs.io/en/latest/py_tutorials/py_imgproc/py_canny/py_canny.html). [Accessed: March 2018].
- [33] V. Jaimini, “Hackerearth.com flood fill tutorial,” 2017. Available: <https://www.hackerearth.com/practice/algorithms/graphs/flood-fill-algorithm/tutorial/>. [Accessed: March 2018].
- [34] E.-M. Nosal, “Flood-fill algorithms used for passive acoustic detection and tracking,” in *New Trends for Environmental Monitoring Using Passive Systems, 2008*, pp. 1–5, IEEE, 2008.
- [35] OpenCV Documentation, “Opencv: ffilldemo.cpp,” 2017. Available: [https://docs.opencv.org/3.3.0/d5/d26/ffilldemo\\_8cpp-example.html](https://docs.opencv.org/3.3.0/d5/d26/ffilldemo_8cpp-example.html). [Accessed: March 2018].
- [36] G. Bradski and A. Kaehler, *Learning OpenCV: Computer vision with the OpenCV library.* ” O'Reilly Media, Inc.”, 2008.
- [37] OpenCV Documentation, “Canny edge detector,” 2017. Available: [https://docs.opencv.org/2.4/doc/tutorials/imgproc/imgtrans/canny\\_detector/canny\\_detector.html](https://docs.opencv.org/2.4/doc/tutorials/imgproc/imgtrans/canny_detector/canny_detector.html). [Accessed: March 2018].